GL01621

MECHANICS OF LOW-ANGLE NORMAL FAULTING: AN EXAMPLE FROM ROOSEVELT HOT SPRINGS GEOTHERMAL AREA, UTAH

by

Ronald L. Bruhn, Michael R. Yusas and Fernando Huertas
Department of Geology and Geophysics, University of Utah,
Salt Lake City, Utah 84112

ABSTRACT

Roosevelt Hot Springs geothermal area is located in the Mineral Mountains of southern Utah. The geothermal reservoir is formed by systems of faults and joints in Cenozoic plutonic and Precambrian metamorphic rocks. Low-angle denudation faults dipping between 5° and 35° to the west form an important component of the reservoir's structure. These faults developed simultaneously with steeply dipping faults, some of which merge into denudation faults at depth. Hydrothermally altered cataclasite preserved in the fault zones indicates that faulting occurred under brittle conditions in the presence of chemically reactive fluids.

Gently westward dipping joints provided planes of weakness along which the denudation faults nucleated. The average coefficient of sliding friction along the faults was less than 0.5 and probably ranged between 0.15 and 0.4. The maximum depth for formation of the denudation faults was estimated as 4 km.

Hydrothermal alteration along the faults and joints hydrolyzed silicate minerals and also produced phyllosilicates, including clay minerals and sericite. The chemical alteration may have significantly decreased the resistance to sliding. This process was a necessary prerequisite for the formation of faults dipping as gently as 10°.

Hydrothermal alteration in the present geothermal reservoir is similar to that observed in the exhumed denudation faults, indicating that the frictional resistance along faults and joints in the reservoir could be significantly lower than along similar structures in unaltered granitic rock. Studies of the structural stability of the reservoir as a consequence of fluid withdrawal and reinjection should consider possible mechanical

effects of hydrothermal alteration.

INTRODUCTION

Low-angle normal faulting is commonly associated with Cenozoic deformation in the Basin and Range Province of the western United States (Armstrong, 1971; Davis and Coney, 1978). The faults may develop in either brittle or ductile environments of deformation depending on their depth in the crust and local geothermal gradients. Denudation faults form an important type of low-angle normal fault associated with the movement of cover rocks from uplifting highlands toward adjacent valleys or grabens. Denudation faulting results in extensive brittle deformation in the fault plates with cataclasis, jointing and the development of high-angle normal faults that often merge into gently dipping decollement surfaces at depth.

Information about the frictional behavior of denudation faults is important to solving problems in regional tectonics as well as reservoir engineering. Denudation faulting is common in volcano-tectonic rift provinces, such as the Basin and Range Province. Therefore, understanding the mechanics of these gently dipping normal faults is a fundamental problem in regional tectonics. Also geothermal and petroleum reservoirs may exist in denudation fault plates and the frictional behavior of the faults could strongly affect production-induced seismicity and reservoir stimulation experiments.

Knowledge of the depth at which denudation faulting is initiated has important economic as well as tectonic implications. The intense brittle deformation in the fault plates is ideal for the development of fractured reservoirs that may contain commercial quantities of petroleum or geothermal fluids (Kostura and Ravenscroft, 1977; Nielson and others, 1978). The potential volume of a reservoir will be directly related to the maximum depth of low-angle faulting.

There are several ways to estimate the maximum depth of denudation faulting. In some areas, fault plates derived from an uplifted region are faulted over Cenozoic valley

fill (Armstrong, 1971). Knowledge of the local stratigraphy can then be used to estimate the original thickness of the plate or stack of fault plates, whichever is the case. In other areas, the position of the basal fault is not certain and one must either directly or indirectly measure the thickness of the zone of faulting using geological or geophysical techniques. Alternatively, one may attempt to use calculations based on known rock properties and mechanical principles to constrain the maximum depth of faulting in a specific environment. This latter approach may aid in the interpretation of geological and geophysical surveys made in the terrane.

Recent advances in our knowledge of rock properties and the magnitudes of stress in the crust provide new impetus to investigate the mechanics of low-angle normal faulting. An extensive amount of information is now available from laboraory testing concerning rock properties under brittle conditions and, in particular, the behavior of anisotropic rocks containing crack arrays, joints and faults (Paterson, 1978; Logan, 1980). Furthermore, the results of field studies in part of the Basin and Range Province suggest that laboratory data can be successfully extrapolated to geological environments in the upper crust (Zoback and Zoback, 1980). Finally, the results of many stress measurements allow one to estimate stress gradients at depths up to several kilometers (Jamison and Cook, 1980; McGarr, 1980).

GEOLOGY OF ROOSEVELT HOT SPRINGS GEOTHERMAL SYSTEM

Roosevelt Hot Springs geothermal area is located in the west-central flank of the Mineral Mountains of southern Utah (Figure 1). The mountain range is formed by a Tertiary felsic plutonic complex that was intruded into Precambrian metamorphic rock and Paleozoic strata (Earl, 1957; Liese, 1957; Condie, 1960; Sibbett and Nielson, 1980).

The geothermal reservoir is formed by a complex system of faults and joints that developed in the Precambrian and Cenozoic crystalline rocks after consolidation of the plutonic complex (Lenzer and others, 1976; Ward and others, 1978, Nielson and others,

1978). Nielson and others (1978) suggest that much of the reservoir's permeability was developed by refracturing of older denudation fault zones during the more recent, high-angle normal faulting.

Low to moderate angle denudation faults occur throughout the Mineral Mountains but are most common in the geothermal area along the west-central flank of the range (Sibbett and Nielson, 1980). The faulting post-dated granitic dikes intruded 12-13 m.y. ago (Evans, 1980) and pre-dated the extrusion of rhyolitic domes and flows dated at 0.4-0.5 m.y. (Evans and Nash, 1978). Most denudation faults in the geothermal area dip toward the west between 5° and 35° in Precambrian metamorphic and Tertiary plutonic rock (Figure 2). Some of these faults have listric geometries with the dip steepening up-section to as much as 65° (Nielson and others, 1978). The denudation fault plates are cut by numerous northwest trending faults that dip between 70° and 90° (Figure 1, 2). Many of these faults root in denudation fault zones at depth, proving that movements on the high and low-angle faults occurred simultaneously (Nielson and others, 1978). The fault plates also contain many small, gently to moderately westward dipping faults that formed by shearing along joints.

The amount of displacement on the faults is generally difficult to determine due to the lack of marker units in the crystalline rock. The geometry of the denudation faults and the associated high-angle fault set indicates that movement was toward the west or southwest. This direction of movement is also indicated by slickenside orientations in many of the smaller fault zones (Yusas and Bruhn, 1979). Nielson and others (1978) estimated 610 m of displacement in a $S80^{\circ}W$ direction from offset lithologies on part of a large denudation fault at a locality just south of the geothermal area. Displacements on many of the smaller faults formed by structurally reactivated joints are likely to be several meters or less.

The faults contain hydrothermally altered cataclasite in zones up to 15 m thick indicating that deformation proceeded under brittle conditions. The most abundant

alteration minerals are clays, sericite, chlorite and epidote. In some areas, micro-diorite and rhyolite dikes were injected along the faults and subsequently deformed as the result of renewed movement (Nielson and others, 1978; Yusas and Bruhn, 1979).

The youngest faults in the geothermal area consist of steeply dipping normal faults that locally cut Quaternary deposits (Figure 1; Petersen, 1975). Another set of faults trends eastward, cutting across the strike of the mountain range. Little is known about the history of this latter fault set, although east trending faults may form important structures in the geothermal reservoir (Ward and others, 1978).

Joints represent an important component of the reservoir's structure and provide passageways for water infiltrating into the geothermal system. The joint system is relatively homogeneous throughout the central Mineral Mountains; generally consisting of three major joint sets (Figure 3, 4; Yusas and Bruhn, 1979). Two sets of steeply dipping, sub-orthogonal extension joints trend northward and eastward, occurring roughly parallel and perpendicular to the strike of the contacts between the igneous and country rocks. Joint spacing is variable, ranging from 1 m to 30 m in the more structurally coherent parts of the plutonic complex to less than a centimeter in areas where intense faulting has occurred (Yusas and Bruhn, 1979). In these latter areas, many of the joints have undergone shear displacements and now consist of hydrothermally altered, anastomosing fractures with slickensided surfaces.

The third major joint set consists of gently to moderately westward dipping joints that generally have smooth, planar surfaces (Figure 3, 4). Joint spacing ranges from 0.1 to 1.0 m in unfaulted parts of the plutonic complex to as little as 10 cm in highly faulted regions. In these latter areas, the joints sub-parallel the denudation faults and many of them contain hydrothermally altered cataclasite formed by shearing.

It is important to note that the joint system in the Precambrian rocks is similar to that in the pluton. This indicates that the ancient and complex structural fabrics in the metamorphic rocks did not control joint attitudes.

We determined the micro-crack fabric in quartz grains from a number of samples collected in the plutonic complex and Precambrian country rock. The fabrics are orthorhombic and consistently oriented between the various sites. There is good correlation between the orientations of micro-cracks and joints in outcrops from which the samples were collected (Figure 5). Orthorhombic crack fabrics are often found in crystalline rocks and presumably reflect the effects of applied and residual stress release during uplift and decompression (Scholtz and Kazinski, 1979). Notably, principal residual stress orientations in outcrops of Mineral Mountains' granite and gneiss generally correspond with joint orientations, and, to a lesser degree, with the micro-crack orientations (Fig. 5; Yusas and Bruhn, 1979).

MECHANICS OF LOW-ANGLE NORMAL FAULTING

Stress orientations: The Late Cenozoic stress field in the Mineral Mountains has been extensional with a vertical maximum principal compressive stress (σ_1) and a west to southwest trending minimum principal compressive stress (σ_3). The mountain range is located in the transition zone between the Basin and Range Province and Colorado Plateau (Figure 1, Stokes, 1979). Regional extension in this part of the transition zone may have begun as early as 26 m.y. ago and was certainly underway by 20 m.y. ago (Rowley and others, 1978). The onset of extension was marked by an abrupt change from regional calc-alkaline volcanism to bi-modal basalt-rhyolite volcanism accompanied by the formation of north-trending horsts and grabens. This style of tectonism, which indicates a regionally vertical σ_1, has continued to the present.

The orientations of igneous dikes, faults and aligned rhyolite domes in the Mineral Mountains indicate that since at least 12 m.y. ago the local stress field was similar in orientation to the regional field (Table 2). This means that the denudation faults apparently formed at angles in excess of 45° to σ_1; at much larger angles than are commonly observed in rock deformation experiments (Paterson, 1978) and field studies

(Hobbs and others, 1976).

Information about the angle between paleo- σ_1 and a specific fault can be determined from the attitudes of extension fractures in the wall rock, because σ_1 was oriented down the dip of the north trending extension fractures that developed during faulting while σ_3 was perpendicular to them. We have studied the extension fractures at several locales where a denudation fault is exposed. In general, the extension fractures in the wall rock dip between 70° and 90° west, regardless of the dip of the fault. This indicates that the angle between σ_1 and the segments of denudation faults dipping 10° to 20° west was as large as 70° to 80°.

Rock properties: A failure envelope for unaltered Mineral Mountain granite is presented in Figure 6. The envelope, which is preliminary, is constructed from the results of three tri-axial compression tests by Pratt and Simonson (1976) and tensile strength tests by Yusas and Bruhn (1979). The cohesive strength (C) is 20 MPa and the coefficient of internal friction (μi) ranges between 1.6 and 0.6 with increasing confining pressure. The uniaxial compressive strength (So) is 121 MPa.

A tensile strength of 5 $\pm$2.4 MPa was determined from twenty Brazil tests on samples collected by Yusas and Bruhn (1979). The large standard deviation in the test results reflects a strong grain size dependence in tensile strength. Eight of the samples had average grain diameters of 1 mm and an average strength of 6.9 $\pm$ 1.7 MPa, while the other samples with 2 mm average grain dimensions had a tensile strength of only 2.5 $\pm$ 0.6 MPa. Presumably, this decrease in strength with increased grain size reflects the presence of longer flaws or cracks in the larger grains (Brace, 1964). Griffith crack theory predicts that the rock with bigger grains should be weaker; as is commonly observed in strength tests.

There are several lines of evidence suggesting that the failure envelope (Figure 6) is sufficiently representative of the different igneous and metamorphic rocks in the Mineral Mountains to justify its use in investigating the tectonics of denudation faulting. Firstly,

the envelope's general shape and the magnitudes of the parameters C, μ_i and So are well within the range of test results on common quartzo-feldspathic igneous and metamorphic rocks (Obert and Duvall, 1967; Jaeger and Cook, 1976). Secondly, the youngest normal faults along the western flank of the range dip between 70° and 75° to depths of at least a kilometer (Figure 2). This dip angle would correspond to internal friction coefficients (μi) of 1.19 to 1.73 for the metamorphic and igneous rocks cut by the faults. These values are in agreement with the experimentally determined value of 1.6 (Figure 6) for the granite samples at low confining pressure. Also, it should be noted that the joint and micro-crack fabrics in the granitic rocks are identical to those in the Precambrian gneiss, and the results of Brazil tests on Precambrian gneiss with 1 mm average grain dimensions gave an average tensile strength of 6.7 ± 0.6 MPa for four samples; essentially identical to the tensile strength of the igneous rocks with similar grain sizes (Yusas and Bruhn, 1979).

Compositionally, most of the igneous and metamorphic rocks in the mountain range are quartzo-feldspathic and individual samples from one phase often overlap in composition with those of other phases (Nielson and others, 1978). This similarity in composition is probably the underlying cause for the relatively homogeneous mechanical properties inferred from the field and laboratory data. It should be noted, however, that Nielson and others (1978) found a greater intensity of faulting in the Tertiary hornblende gneiss than in other units and the amount of cataclasis was much less in the biotite-rich gneisses than in the other rocks.

Fault mechanics: Hypotheses for the origin of denudation faulting must account for the simultaneous evolution of the denudation faults, the northwest striking faults that dip steeply between 70° and 90° (Figure 2) and the locally intensive shearing along the gently westward dipping joint set. If σ_1 was vertical, as we have inferred from geological data (Table 1), then the steeply dipping faults could be predicted given the failure envelope in Figure 6 and sufficient shear stresses to cause faulting. However, the gently

dipping denudation faults would not be expected to develop.

The fact that steeply dipping faults formed during denudation faulting places an important constraint on the nature of the deviatoric stresses. In some areas the steeply dipping faults cut across vertical extension fractures, indicating shear failure of the rock. But, in other localities, the extension joints contain cataclasite, suggesting that extensional failure was followed by shearing. In either case, the deviatoric stresses must have been of sufficient magnitude to cause the simultaneous development of both high and low-angle faults.

The most probable explanation for the development of faults at angles greater than 45° to σ_1 is that the rock was anisotropic, with preferentially oriented planes of weakness. Either joints or planar arrays of micro-cracks are the most probable causes of such strength anisotropy in crystalline rocks (Walsh and Brace, 1964; Jaeger and Cook, 1976; Paterson, 1978). We suggest that the gently to moderately westward dipping joints and micro-crack arrays in the Mineral Mountains formed planes of weakness along which the denudation faults nucleated. This would explain why many of the gently dipping joints have locally undergone shearing, particularly in the vicinity of major denudation faults.

Shearing along faults or joints will be greatly facilitated by excessive pore fluid pressures (Hubbert and Rubey, 1959). However, we suspect that the average pore pressure during denudation faulting was near the hydrostatic value. This arises from the observation that extensive jointing and high-angle faulting occurred simultaneously with movement on the denudation faults. The process of continued fracturing in the denudation fault plates should have progressively increased the fracture permeability of the rock, and consequently, maintained the pore pressure near hydrostatic.

The potential effects of rock friction on the mechanics of denudation faulting can be investigated using experimentally derived data on the frictional properties of joints and

faults. Coefficients of friction for sliding along pre-cut surfaces in felsic rocks generally vary between 0.5 and 0.8 (Jaeger and Cook, 1976; Paterson, 1978) and between 0.6 and 1.0 for sliding on artificially formed shear surfaces (Paterson, 1978). The equation that is most representative for repeated sliding on pre-existing surfaces is $\tau_s = 0.85\ \sigma_n$, where τ_s = shear stress to initiate sliding and σ_n = effective normal stress across the surface (Byerlee, 1978). This equation holds over large ranges in rock composition, gouge thickness, confining pressure, pore pressure, temperature and strain rate in the laboratory at normal stresses to 2 Kb. If $\sigma_n \geq 2$ Kb, μ_s is estimated as 0.6.

Jamison and Cook (1980) have used the results of stress tests in the uppermost crust to estimate the cohesive strengths and friction coefficients of natural faults and joints. They found that the cohesive strength (C) was nearly zero and that coefficients of sliding friction (μ_i) ranged between 0.22 and 0.65.

The work of Byerlee (1968) and Jamison and Cook (1980) suggests that we need to consider the effects of varying the friction coefficient between 0.85 and 0.2 in controlling the orientations of denudation faults. The strength of an anisotropic rock varies as a function of the angle (Θ) between σ_1 and the weakness plane (Jaeger and Cook, 1976). The differential stress needed to fail the rock can be found from the following equation which is derived from the discussion of Jaeger and Cook (1976, p. 25-26).

$$(1) \quad (\sigma_1 - \sigma_3) = \sigma_1 \left[1 - \frac{(1 - \mu_s \cot 2\theta - \mu_s / \sin 2\theta) - 2C/\sin 2\theta}{(1 - \mu_s \cot 2\theta + \mu_s / \sin 2\theta)} \right]$$

In this equation C is the cohesive strength and μ_s the coefficient of sliding friction for the plane of weakness; θ is the angle between σ_1 and the perpendicular to the plane. If σ_1 is vertical, as assumed in this study, then θ is also the dip angle of the plane of weakness.

The rock strength given by equation (1) can be normalized with respect to the

strength given by the failure envelope (Figure 6) for coherent rock lacking a throughgoing anisotropy plane and plotted against θ to produce the curves shown in Figure 7. These curves represent several different values for the friction coefficient (μ_s) on the weakness plane and show how the normalized strength of the rock ($\Delta\sigma^*$) varies as a function of the dip angle of the anisotropy plane (σ_1 is assumed to be vertical).

A graph like that in Figure 7 can be constructed for any depth of interest if the vertical shear stress and pore pressure gradients are known. McGarr (1980) reports maximum shear (τ_{max}) stress variations with depth in crystalline rock based on hydrofracture stress tests. The equation $\tau_{max} = A + Bz$ can be fitted to hydrofracturing data, where A and B are constants and Z is depth in kilometers. For 15 measurements in extensional regions A = 1.00 $\pm$ 3.76 MPa and B = 6.69 $\pm$ 1.93 MPa/km while the average values for 59 measurements from both extensional and compressional regimes are A = 5 $\pm$ 1.15 MPa and B = 6.59 $\pm$ 0.95 MPa/km. Consequently, we assume that $\tau_{max} \sim 1\,MPa + 7\,MPa/Km$ the paleo-shear stress in the Mineral Mountains can be estimated from the equation for extensional regions. Also, we suggest that the pore pressure values included in our calculations must be nearly hydrostatic based on the geological arguments discussed previously. Notice that Figure 7 has been constructed for a depth of 2 km. A pore pressure equal to 125% of the hydrostatic value is required to cause high and low-angle faulting simultaneously.

The curves in Figure 7 can be used to determine the minimum dip angle (θ min) for an anisotropy plane along which sliding can occur given a specific coefficient of friction. This is due to the fact that high-angle normal faulting occurred in the denudation fault plates simultaneously with slip on the denudation faults. Mechanically, this means that the intersection of the U-shaped strength curve with the line $\Delta\sigma^* = 1$ lies directly above the minimum possible dip angle (θmin) for a low-angle fault. For example, θmin in Figure 7 is $\sim 5.5^\circ$, 14° and 22° for faults with friction coefficients (μs) of 0.1, 0.3 and 0.5, respectively.

We constructed graphs like Figure 7 for depths between 2 km and 5km with friction coefficients ranging between 0.1 and 0.6. In each case we determined θ min and listed the results in Table 2. The minimum depth of 2 km was selected because the known thicknesses of preserved fault plates is about 1.5km (Nielson and others, 1978). The pore pressure needed to initiate high-angle faulting at any depth is limited by the geometry of the failure envelope for intact rock and the principal stress difference, which is fixed by the assumed shear stress gradient.

Inspection of Table 1 shows that $\mu_s \geq 0.5$ is too large, because there is field evidence that the angle between σ_1 and some of the larger denudation faults was 70° or greater, requiring that $\theta min \leq 20^\circ$. An upper bound for the friction coefficient must be in the range $0.4 \leq \mu_s \leq 0.5$. . This upper bound is much lower than the commonly cited values of $\mu_s \geq 0.6$ found for sliding on faults in the laboratory (Byerlee, 1978) but is within the range of friction coefficients estimated from stress tests (Jamison and Cook, 1980).

We have attempted to estimate a lower bound for the friction coefficient by calculating the resisting forces acting on one of the preserved denudation fault plates (Fig. 2). The two-dimensional geometry and dimensions of the plate (Fig. 8) are taken from cross section B-B' of Nielson and others (1978). The basal denudation fault has been offset along younger, high-angle faults, but we suggest that the numerous low-angle joints in the fault plate probably provide potential slip-surfaces connecting the larger segments of the old fault. The subsurface structure along the western margin of the mountain range is from the seismic refraction work of Gertson and Smith (1979). The pore pressure in the geothermal field is assumed to be hydrostatic.

The method of analysis is a modification of Janbu's (1954) "method of slices" for calculating the factor of safety on a non-circular fault. We have introduced new terms into Janbu's original equations to account for the effects of tectonic shear stresses and resisting forces due to abutting of the fault plate against valley fill (Appendix 1). The

coefficient of friction is found by setting the gravitational and tectonic driving forces equal to the resisting forces caused by the weight of the valley fill and frictional resistance along the non-circular fault surface. This assumes that the fault plate is in static equilibrium because there is no geological evidence for contemporary movement on the low-angle fault. Satisfying the assumption provides a lower bound estimate for the friction coefficient (μ_s), if the cohesion of the fault is negligible. The calculation suggests that $\mu_s = 0.3$ is a reasonable estimate for a lower bound on the coefficient of friction, but we must emphasize that a large number of assumptions were required to arrive at this estimate. If tectonic stresses are not considered, $\mu_s > 0.15$ (Table 3) We suggest, then, that the coefficient of sliding friction along the denudation faults was on the average, less than 0.5 and probably greater than 0.15

The data in Table 2 can be used to estimate the maximum depth for denudation faulting. Unfortunately, the assumed shear stress gradient during faulting is speculative and θ min is a slowly varying function of depth. Therefore, the "maximum depth of faulting" estimate is poorly constrained. Large segments of the denudation faults apparently formed at angles between 70° and 80° to σ_1 ; this corresponds to θ min as small as 10°. If the coefficient of sliding friciton (μ_s) was ≈0.2or greater, then the maximum depth of faulting was probably constrained to depths at or above 4 km (Table 2).

DISCUSSION

The suggestion that the very gently dipping denudation faults formed at depths above 4 km agrees with the results of a magnetotelluric survey in the geothermal area by Wannamaker and others (1980), who concluded that a marked decrease in the intensity of fracturing presently occurs at a depth between 1.5 and 2 km. Also, the seismc refraction study of Gertson and Smith (1979) indicated a marked increase in p-wave velocity from 4.0 km/sec to 5.5 km/sec at depths of 1.5 to 2 km. Their result seems consistent with an abrupt decrease in fracture intensity at depth although part of the refraction profile was

located along a major east-trending vertical fault and thus the velocity structure may not be representative of the denudation fault system. The transition in the intensity of fracturing with depth may represent the preserved lower boundary for denudation faulting.

Nielson and others (1978) suggested that plates of crystalline rock could have been faulted over valley fill along some of the denudation faults. We have not taken topographic stresses into account in this study since the paleo-topography of the mountain range and its history of uplift are not known with any certainty. However, the shallow depths at which denudation faulting is expected to occur and the relatively low coefficients of sliding friction that we have estimated suggest that their hypothesis is mechanically feasible. This is not surprising, given the fact that crystalline rocks have clearly been emplaced over valley fill by denudation faulting at a number of localities in the western U.S. (Davis and Coney, 1978).

The required pore pressure of 125% hydrostatic to cause faulting is dictated by the experimental failure envelope (Fig. 6) and the assumed shear stress gradient of τ_{max} = 1MPa + 7 MPa/Km. The required pore pressure would be less if the strength of the intact rock was lower than that predicted by the failure envelope. This is likely, since laboratory determined rock strengths are liable to be upper bound values for the strength of rock during natural deformation. However, we could only speculate on what a reasonable modification of the failure envelope should be. Such speculation is not warranted given the additional uncertainty of the "best estimate" shear stress gradient taken from the work of McGarr (1980).

Cataclastite in the major faults and along sheared joint surfaces is hydrothermally altered to assemblages of clay minerals, chlorite, sericite and epidote (Nielson and others, 1978; Yusas and Bruhn, 1980). Inspection of thin sections indicates several phases of mineral growth and fault movement (Nielson and others, 1978; Sibbett and Nielson, 1980) and striated fault surfaces are coated with the alteration minerals. This evidence proves that hydrothermal alteration occurred during faulting. Many of the phyllosilicates

formed by reactions between feldspar and fluid, causing a significant decrease in modal feldspar.

There is experimental evidence suggesting that friction along the joints and faults may have been lowered as the result of hydrothermal alteration. Trace amounts of water have been known to significantly decrease the strength of silicates in both brittle and ductile regimes of deformation (Logan, 1980; Tullis, 1980). Extensive rock-water interaction along joints and faults would hydrolyze silicate minerals and drastically affect the frictional properties of rock. Unfortunately, most laboratory studies of rock friction have not investigated the effects of a chemically reactive fluid phase, although hydrothermal alteration is ubiquitous in many fault zones.

The results of a few laboratory experiments indicate that alteration causing an increase in phyllosilicates accompanied by a decrease in modal feldspar may cause a significant reduction in the resistance of rock surfaces to sliding (Wang and Mao, 1979). Water saturated clays influence sliding behavior in two ways: first, the magnitudes of stresses transmitted through the framework of the mineral grains may be reduced due to the low permeability of phyllosilicate aggregates and secondly, the intrinsic frictional properties of clay particles may be altered by changing the state of hydration of ions on the surface of each particle (Wang and Mao, 1979; Wang, 1980). Laboratory studies on the static and kinetic coefficients of sliding friction of saturated chlorite and muscovite aggregates indicate $\mu_s = 0.26$, about three times less than these coefficients for microcline feldspar ($\mu_s = 0.77$; Horne and Deere, 1962). More recent experiments at confining pressures to 30 MPa by Wang and Mao (1979) indicate $\mu_s = 0.08$, 0.12, 0.15 and 0.22 for sliding on joints filled with saturated montmorillonite, kaolinite, chlorite and illite, respectively. Natural clay gouge from part of the San Andreas fault zone has frictional coefficients of 0.2 to 0.3 in the same types of experiments. It is important to note that these friction coefficients may partly reflect localized, high pore pressures in the saturated mineral aggregates due to their

low permeability; although Wang and Mao's (1979) preliminary conclusion was that their experimental design probably allowed time for the establishment of equilibrium pore pressure between the joint filling and granodiorite test sample. Regardless, these experiments suggest that alteration mineral assemblages like those found in the faults and joints in the Mineral Mountains could drastically reduce the resistance to sliding relative to that along unaltered granitic surfaces. We would expect friction along the natural surfaces to be somewhat higher than indicated by the laboratory experiments on pure phyllosilicate aggregates, given the fact that the observed alteration did not consume all of the host rock and is heterogeneously distributed. Also, any excess pore pressures localized along joints or faults would have much longer times to decay than in laboratory tests.

The rock friction estimates of $\mu_s < 0.5$ have potentially important implications for exploitation of the present geothermal system. Hydrothermal alteration along joints and faults in the geothermal reservoir is continuing at the present and the mineral assemblages are similar to those found in the exhumed denudation faults (Parry and others, 1978). This implies that the resistance to sliding on joints and faults in the reservoir might be considerably lower than in the surrounding unaltered granitic rock. A thorough investigation of the mechanical effects of this alteration is needed in order to aid in engineering studies of the potential structural stability of the reservoir during large scale fluid extraction and re-injection.

CONCLUSIONS

Denudation faults in the Mineral Mountains developed by shearing along an evolving set of gently dipping joints and cracks. The average coefficient of friction along the faults was less than 0.5 and probably in the range of 0.15 to 0.4. The maximum depth for formation of the faults is estimated as 4 Km, although this estimate is poorly constrained.

The estimated friction coefficients are lower than the commonly cited values of $\mu_s \geq 0.6$ determined in laboratory faulting tests. However, our estimates are similar to the range of values cited by Jamison and Cook (1980) for friction on natural faults and joints in the uppermost crust ($0.22 \geq \mu_s \leq 0.65$). We speculate that the resistance to sliding on faults, joints and cracks was reduced by hydrothermal alteration. Chemical reactions between the fluid and wall rock probably resulted in hydrolyzation of silicates, with the potential for drastically altering the mechanical behavior of the minerals. Furthermore, phyllosilicates formed while modal feldspar decreased and there is laboratory evidence suggesting that this process could have resulted in drastic reductions in friction due to ionic repulsion of some clay minerals and localized excessive pore pressures in the phyllosilicate aggregates. Hydrothermal alteration is ubiquitous in many fault zones and much work needs to be done in investigating the effects of chemically reactive fluids on rock friction.

ACKNOWLEDGEMENTS

We thank D. L. Nielson and R. B. Smith for reviewing a preliminary draft of this manuscript. The work was supported by the United States Department of Energy under contract ~~DOE/DGE-ET/28392-31~~ DE-AC07-78ET-28392 and DE-AC07-80ID 12079, and with a grant from the Research Corporation to R. L. Bruhn.

APPENDIX I

An estimate of the lower bound for the static coefficient of sliding friction is found by assuming that the cross-section of the large denudation fault plate in Figure 2 is in static equilibrium. Presumably, the many gently dipping joints in the fault plate provide potential planes of weakness connecting the segments of the fault where it is off-set by younger, normal faults. The fluid pressure is assumed to be hydrostatic and the maximum shear stress at any given depth is estimated from the equation τ_{max} = 1 MPa + 7 MPa/km (McGarr, 1980). The resisting and driving forces are resolved into horizontal components and set equal by adjusting the magnitude of the friction coefficient (μ_s) on the fault using the non - circular fault analysis of Janbu (1954). We have added a term to Janbu's equation to account for tectonic shear stress on the fault plane.

The fault plate is divided into six segments of mean height (h_i), length (Δx_i), and unit width (Fig. 8). The weight per unit volume of crystalline rock is estimated as 26.5 kg/m^3 and that of the alluvium as 22.5 kg/m^3 . The cohesive strength of the fault is considered to be negligible, following the results of Jamison and Cook (1980).

The equation to be solved for μ_s is:

$$\underbrace{\mu_s\left[\sum_{i=1}^{6}\frac{(P_i-u_i)\Delta x_i}{N_i}\right]+R}_{\text{resisting force}} = \underbrace{\frac{1}{f_o}\sum_{i=1}^{6} W_i \tan\alpha_i + \tau_i \sin 2\alpha_i \Delta x_i}_{\text{driving force}}$$

$P_i = \rho_i g h_i$; ρ_i = density and g = |gravitational acceleration|.

U_i = pore pressure at depth h_i .

W_i = weight of segment "i".

α_i = average dip angle of segment "i".

τ_i = maximum shear stress at depth "h_i" found from τ_{max} = 1 MPa + 7 MPa/km.

f_o = correction factor to allow for inter-segment forces. This factor is found by taking the ratio d/L (Fig. 8) and consulting Figure 114 of Hoek and Bray (1977). Here, f_o = 1.013.

$N_i = (1 + \mu_s \tan \alpha_i) \cos^2 \alpha_i$.

R = force due to valley fill abutting against the western end of the fault plate (Fig. 8). $R = \frac{1}{2} W_f Z^2$, where W = average weight per unit volume of the Tertiary and Quaternary valley fill ($\sim$ 23.5 knewtons/m^3). The depth (Z) to the fault is 1070 m.

The tectonic shear stress term ($\tau_i \sin 2\alpha_i \Delta x$) for each segment is found by calculating τ_i for each segment and resolving it to find the shear stress on the fault dipping at angle α_i. The maximum principal compressive stress is assumed to be vertical. The total shear force on the fault segment is $\tau_i \sin 2\alpha_i \Delta x_i / \cos \alpha_i$. The horizontal component of this force is $(\tau_i \sin 2\alpha_i \Delta x_i / \cos \alpha_i) \times (\cos \alpha_i) = \tau_i \sin 2\alpha_i \Delta x_i$. The remainder of the equation is derived and discussed by Janbu (1954) and Hoek and Bray (1977). The results are presented in Table 3.

TABLE I: PALEO-STRESS FIELD AT ROOSEVELT HOT SPRINGS KGRA

TIME	STRESS ORIENTATION	GEOLOGIC EVIDENCE
QUATERNARY	σ_1 - VERTICAL σ_3 - WEST TO WEST-NORTHWEST	NORTH-NORTHEAST STRIKING NORMAL FAULTS IN ALLUVIUM.
0.4-0.5 M.Y.**	σ_3 - EAST-WEST	RHYOLITE DOMES ALIGNED NORTH-SOUTH.
DENUDATION FAULTING	σ_1 - VERTICAL σ_3 - WEST TO WEST-SOUTHWEST	HIGH & LOW-ANGLE NORMAL FAULTS STRIKING NORTH TO NORTH-NORTHWEST.
9 M.Y.*	σ_1 - VERTICAL σ_3 - WEST TO WEST-NORTHWEST	STEEPLY DIPPING RHYOLITE DIKES STRIKING NORTHWARD.
12-13 M.Y.*	σ_1 - VERTICAL σ_3 - WEST TO WEST-NORTHWEST	STEEPLY DIPPING GRANITIC DIKES STRIKING NORTHWARD.

* K/AR DATES FROM EVANS (1980).

** K/AR DATES FROM EVANS AND NASH (1978).

σ_1 - MAXIMUM PRINCIPAL COMPRESSIVE STRESS.

σ_3 - MINIMUM PRINCIPAL COMPRESSIVE STRESS.

TABLE 2: MINIMUM DIP ANGLE FOR DENUDATION FAULTS AS A FUNCTION OF THE COEFFICIENT OF FRICTION AND DEPTH OF FAULTING

DEPTH (Km) \ FRICTION COEFFICIENT (μ_s)	0.1	0.2	0.3	0.4	0.5	0.6
2.0	~5.5°	7°	14°	17°	22°	26°
3.0	6°	9°	15°	18°	23°	27°
4.0	~6.5°	10°	~15.5°	19°	24°	28°
5.5	7°	~10.5°	16°	20°	25°	29°

NOTE: PORE PRESSURE REQUIRED TO CAUSE DENUDATION FAULTING IS ABOUT 125% HYDROSTATIC IF τ_{max} = 1 MPa + 7 MPa/Km.

TABLE 3: LOWER BOUND ESTIMATE FOR STATIC COEFFICIENT OF FRICTION

Case 1: τ max = 1 MPa + 7 MPa/km

Coefficient of friction (μ_s)	Ratio of resisting to driving forces **
0.1	0.2
0.2	0.6
0.3	0.8
0.4	1.1
0.5	1.3

Case 2: We set tectonic stresses equal to zero and consider only body forces.

Coefficient of friction (μ_s)	Ratio of resisting to driving forces **
0.1	0.5
0.15	0.9
0.2	1.3

** NOTE: The ratio of resisting to driving force equals one if the fault is in static equilibrium. Thus, for case 1 μ_s is greater than 0.3 while for Case 2 μ_s is greater than 0.15.

REFERENCES

Armstrong, R. L.. 1971. Low-angle (denudation) faults, hinterland of the Sevier Orogenic Belt, eastern Nevada and western Utah. Geol. Soc. America Bull., 83: 1729-1754.

Brace, W. F., 1961. Dependence of fracture strength of rocks on grain size. Proc. 4th Symp. Rock Mechanics, Penn. State Univ. Min. Ind. Exp. Sta. Bull., No. 76: 99-103.

Byerlee, J. D., 1978, Friction of rocks, Pure and Applied Geophysics, v. 116: p. 615-626.

Condie, K. C., 1960, Petrogenesis of the Mineral Range pluton, southwestern Utah. Univ. of Utah, M.S. thesis: 92 p.

Davis, G. H., and Coney, P. J., 1979. Geologic development of the metamorphic core complexes. Geology, 7, 120-124.

Earll, F. N., 1957. Geology of the central Mineral Range, Beaver County, Utah. Univ. of Utah, Ph.D. thesis: 112 p.

Evans, S. H., Jr., 1980. Summary of potassium/argon age dating - 1979. DOE/DGE report Contract DE-AC07-78ET/28392: University of Utah, Department of Geology and Geophysics, Salt Lake City, Utah, 23p.

Evans, S. H., Jr., and Brown, F. H., 1980. Summary of potassium/argon age dating - 1980. DOE/DGE report, Contract DE-AC07-80ID12077, University of Utah, Department of Geology and Geophysics, Salt Lake City, Utah: 23 p.

Evans, S. H., Jr., and Nash, W. P., 1978. Quaternary rhyolite from the Mineral Mountains, Utah, U.S.A. DOE/DGE report, Contract EY-76-S-07-1701, University of Utah, Department of Geology and Geophysics, Salt Lake City, Utah.

Gertson, R. C., and Smith, R. B., 1979. Interpretation of a seismic refraction profile across the Roosevelt Hot Springs, Utah and vincinity. DOE/DGE report, Contract DE-AC07-78ET28392, University of Utah, Department of Geology and Geophysics, Salt Lake City, Utah: 116 p.

Hobbs, B. E., Means, W. D., and Williams, P. F., 1976. An outline of structural Geology. (New York, John Wiley and sons): 571 p.

Horn, H. M., and D. V. Deere, 1962, Frictional characteristics of minerals. Geotecnique. 12: 319-335.

Hubbert, M. K., and Rubey, W. W., 1959, Role of fluid pressure in mechanics of overthrust faulting. Geol. Soc. America Bull. 70: p. 115-166.

Jaeger, J. C., and Cook, N. G. W., 1976, Fundamentals of Rock Mechanics. (New York, Halsted Press): 584 pp.

Jamison, D B., and N. G. W. Cook, 1980. Note on measured values for the state of stress in the Earth's crust. J. Geophy. Res. 85: 1833-1838.

Janbu, N., 1954, Application of composite slip circles for stability analysis. Proc. European Conference on stability of Earth Slopes, Stockholm. 3: 43-49.

Heck, E. and Bray, J. W., 1977. Rock Slope Engineering. (London, Institution of Mining and Metallurgy): 401 p.

Kastura, J. R., and J. H. Ravenscroft, 1977. Fracture Controlled Production. Amer. Assoc. Pet. Geol. Reprint Series, No. 21: 221 p.

Lenzer, R. C., Cosby, G. N., and Berge, C. W., 1976. Geothermal exploration of the Roosevelt Hot Springs KGRA. Proc. of the Int. Soc. Rock Mech: 3B1-1.

Liese, H. C., 1957, Geology of the northern Mineral Range, Millard and Beaver counties, Utah. University of Utah, unpublished M.S. thesis: 88p.

Logan, J. M., 1979. Brittle phenomena. Rev. Geophys. Space Phys. 17: 1121-1132.

McGarr, A., 1980. Some constraints on shear stress in the crust from observations and theory. J. Geophs. Res. 85: 6231-6238.

McGarr, A., and Gay, N. C., 1978. State of stress in the earth's crust. Ann. Rev. Earth Planet. Sci. 6: 405-436.

Nielson, D L., B. S. Sibbett, D. B. McKinney, J. B. Hulen, J. N. Moore and S. M. Samberg, 1978. Geology of Roosevelt Hot Springs KGRA, Beaver County, Utah. DOE/DGE report, contract EG-78-C-07-1701, Earth Science Lab., Salt Lake City, Utah: 120 p.

Obert, L., and Duvall, W. I., 1967. Rock mechanics and the design of rock structures.

(New York, John Wiley and Sons): 650 p.

Parry, W. T., Bryant, N. L., Dedolph, R. E., Ballantyne, J. M., Ballantyne, G. H., Rohrs, D. T., and Mason, J. L., 1978. Hydrothermal alteration at the Roosevelt Hot Springs thermal area, Utah. DOE/DGE report, Contract IDO/78-1701.a.1.1., University of Utah, Department of Geology and Geophysics, Salt Lake City, Utah: 29p.

Paterson, M S., 1978. Experimental Rock Deformation: The Brittle Field. Springer-Verlag, N.Y.: 254p.

Peterson, C. A., 1975. Geology of the Roosevelt Hot Springs area, Beaver County, Utah. Utah Geology. 2: 109-116.

Pratt, H. R., and Simonson, E. R., 1976. Geotechnical studies of geothermal reservoirs. Report to Energy Resources Development Agency: 30-34.

Roeder, P., and Witherspoon, W. D., 1978. Palinspastic map of east Tennessee. Amer. Jour. Science. 278: 543-550.

Rowley, P. D., Anderson, J. J., Williams, P. L., Fleck, R J., 1978. Age of structural differentation between the Colorado Plateaus and Basin and Range Province in southwestern Utah. Geology. 6: 51-55.

Scholz, C. H., and Koczynski, T. A., 1979. Dilatancy anisotropy and the response of rock to large cyclic loads. J. Geophys. Res. 84: 5525-5534.

Sibbett, B. S., and Nielson, D. L., 1980. Geology of the central Mineral Mountains, Beaver County, Utah. DOE/DGE report, Contract DE-AC07-78Et28392, Earth Science Lab., Salt lake City, Utah: 42 p.

Tullis, J. A., 1979. High temperature deformatin of rocks and minerals. Rev. Geophys. Space Phys. 17: 1137-1154.

Walsh, J. B., and W. F. Brace, 1964. A fracture criterion for brittle anisotropic rock. J. Geophys. Res. 69: 3449-3456.

Ward, S. H., Parry, W. T., Nash, W. P., Sill, W. R., Cook, K. L., Smith, R. B., Chapman, D. S., Brown, F. H., Wheland, J. A., and Bowman J. R., 1978. A summary of the

geology, geochemstry and geophysics of the Roosevelt Hot Springs thermal area, Utah. Geophysics 43: 1515-1542.

Wang, C., 1980, Sediment subduction and frictional sliding in a subductin zone. Geology, 8: 530-533.

Yusas, M. R., and R. L., Bruhn, 1979. Structural fabric and in-situ stress analyses of the Roosevelt Ht Springs KGRA. DOE/ET report, Contract DE-AC07-78ET28392, University of Utah, Department of Geology and Geophysics, Salt Lake City, Utah: 62 p.

Wang, C. and N. Mao, 1979. Shearing of saturated clays in rock joints at high confining pressures. Geophys. Res. Letters. 6: 825-829.

Wannamaker, P. E., Ward, S. H., Hohmann, G. W., and Sill, W. R., 1980. Magnetotelluric models of the Roosevelt Hot Springs thermal area, Utah. DOE/ET report, Contract DE-AC07-79ET27002, University of Utah, Department of Geology and Geophysics, Salt Lake City, Utah: 213 p.

Zoback, M. L., and M. D. Zoback, 1980. Faulting patterns in north-central Nevada and strength of the crust. J. Geophys. Res. 85: 275-284.

FIGURE CAPTIONS

Figure 1. Location map of Mineral Mountains and geologic map of Roosevelt Hot Springs geothermal area. Geology after Evans and others (1978) and Nielson and others (1978).

Figure 2. East-west cross section across part of Roosevelt Hot Springs geothermal area (after Nielson and others, 1978). Small cataclastic zones are schematic. The line of section is indicated in Figure 1.

Figure 3. Summary diagram of average joint orientations in the central Mineral Mountains. Each field contains the average joint orientations for several domains of similar structure. The data represents over 2000 measurements that are reported in Yusas and Bruhn (1979). Data are plotted on a lower hemisphere, stereographic projection.

Figure 4. Cartoon showing the typical joint and mesoscopic fault geometry in the Roosevelt Hot Springs geothermal area. Note the increased intensity of fracturing adjacent to the faults.

Figure 5. Relations between the orientations of joints and microfractures in granite and gneiss outcrops. The data are plotted on lower hemisphere stereographic projetions and contoured by the Schmidt method. Contour intervals in percent per 1% area are: a, c, e = 1, 2, 3 and 5%, b & d = 1, 4, 8 and 12% and f = 1, 5, 9, and 15%. The maximum horizontal extension axes determined from in-situ residual stress tests are indicated by the large arrows. The original data may be found in Yusas and Bruhn (1979).

Figure 6. Failure envelope for unaltered Mineral Mountain's granite. Compression tests by Pratt and Simonson (1976) and tension tests by Yusas and Bruhn (1979).

Figure 7. Estimated strength of Mineral Mountain granitic rock containing anisotropy planes with zero cohesion and friction coefficients between 0.1 and 0.5. $\Delta\sigma^*$ is the strength $(\sigma_1-\sigma_3)$ of the anisotropy plane divided by the strength of intact rock that

lacks a through-going plane of weakness. This latter strength is represented by the failure envelope in Figure 6. The Figure is discussed in the text.

Figure 8. Fault plate geometry used to calculate the lower bound coefficient of fricition (μ_s) . The figure is discussed in the text and Appendix 1.

FIG.

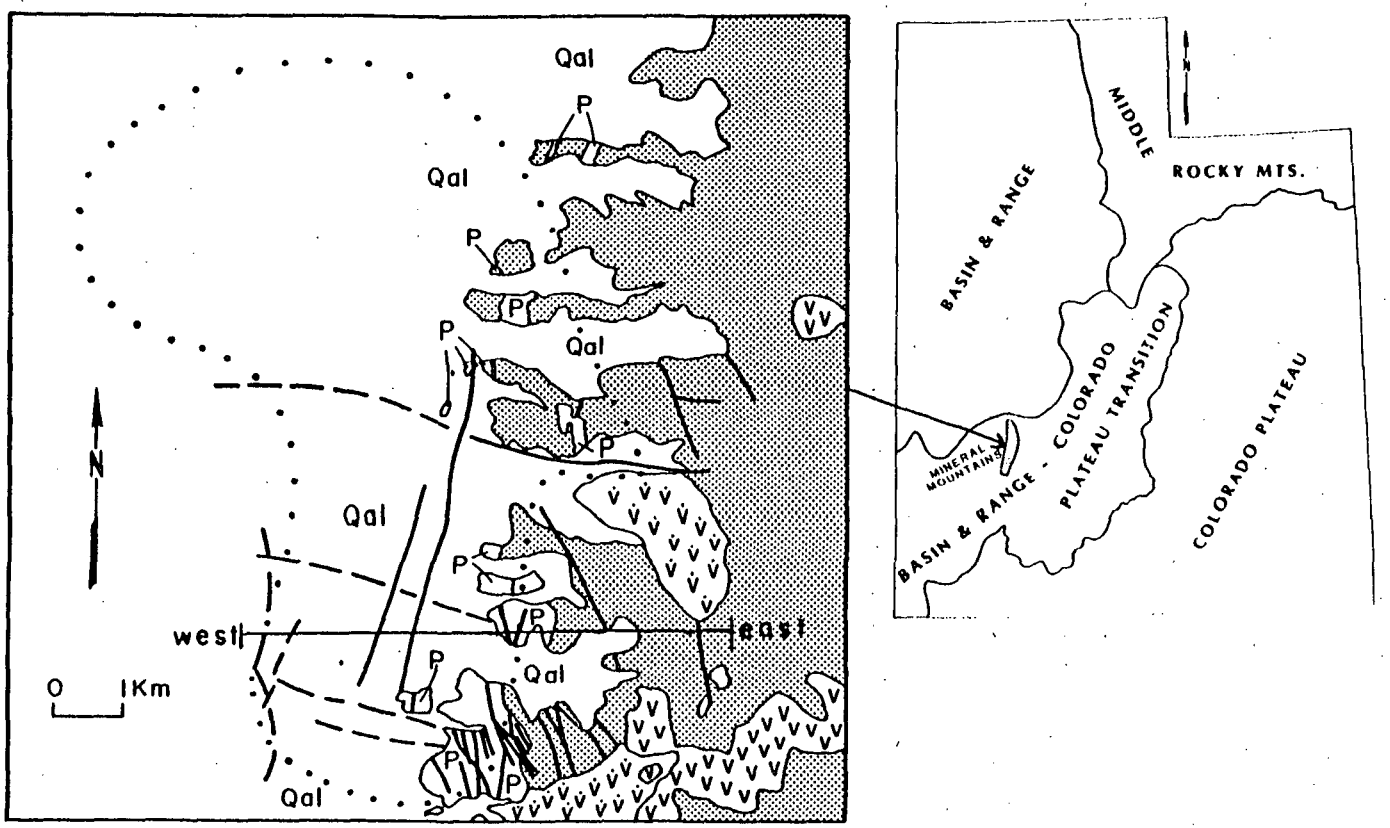

LEGEND

Qal = QUATERNARY DEPOSITS

v̇ = RHYOLITE FLOWS & PYROCLASTICS

v = RHYOLITE DOMES

P = PRECAMBRIAN GNEISS & SCHIST

TERTIARY FELSIC PLUTONS

FAULTS, DASHED WHERE CONCEALED OR INFERRED

400 mWm^{-2} HEATFLOW CONTOUR

FIG. 1

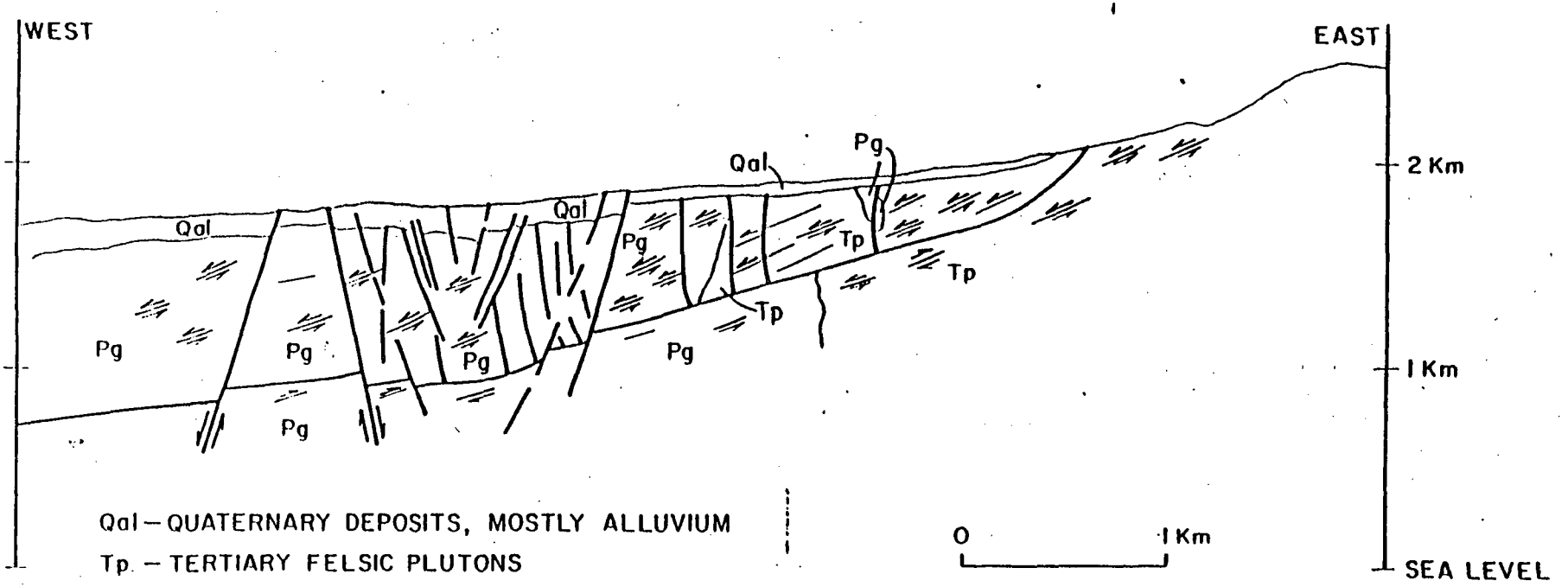
WEST
EAST
Qal
Pg
Tp
2 Km
1 Km
SEA LEVEL
0
1 Km
Qal—QUATERNARY DEPOSITS, MOSTLY ALLUVIUM
Tp—TERTIARY FELSIC PLUTONS
Pg—PRECAMBRIAN GNEISS & SCHIST
—LOW-ANGLE CATACLASTIC ZONES, ARROWS INDICATE INFERRED SENSE OF DISPLACEMENT
—MAJOR FAULTS, ARROWS INDICATE SENSE OF DISPLACEMENT

FIG. 2

FIG. 3

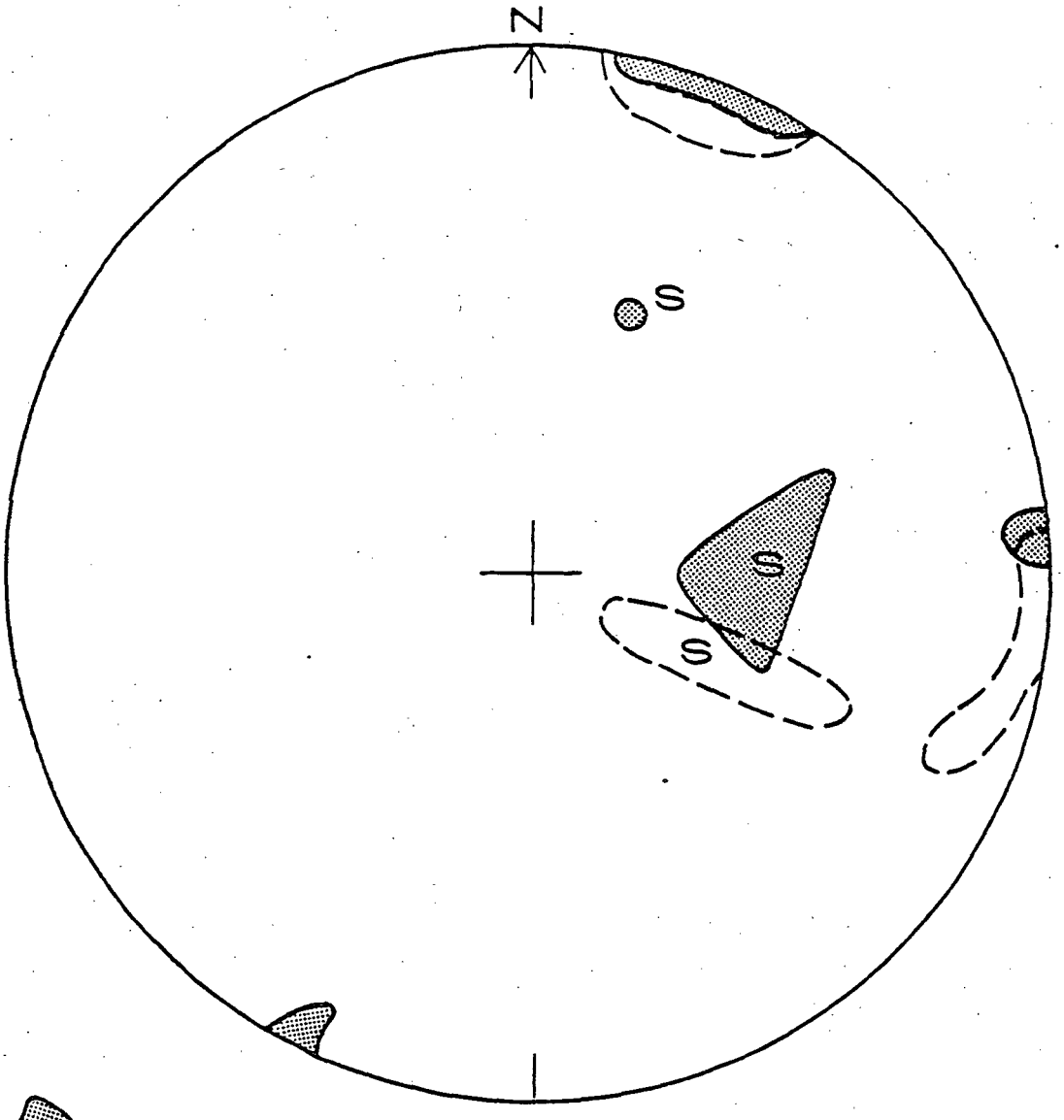

- FIELDS OF AVERAGE JOINT PLANE POLES IN GEOTHERMAL AREA (3 DOMAINS)

- FIELDS OF AVERAGE JOINT PLANE POLES IN PLUTON'S INTERIOR (3 DOMAINS)

S - JOINT SETS CONTAIN CATACLASITE

Fig. 4

FRACTURE SYSTEM IN ROOSEVELT GEOTHERMAL AREA

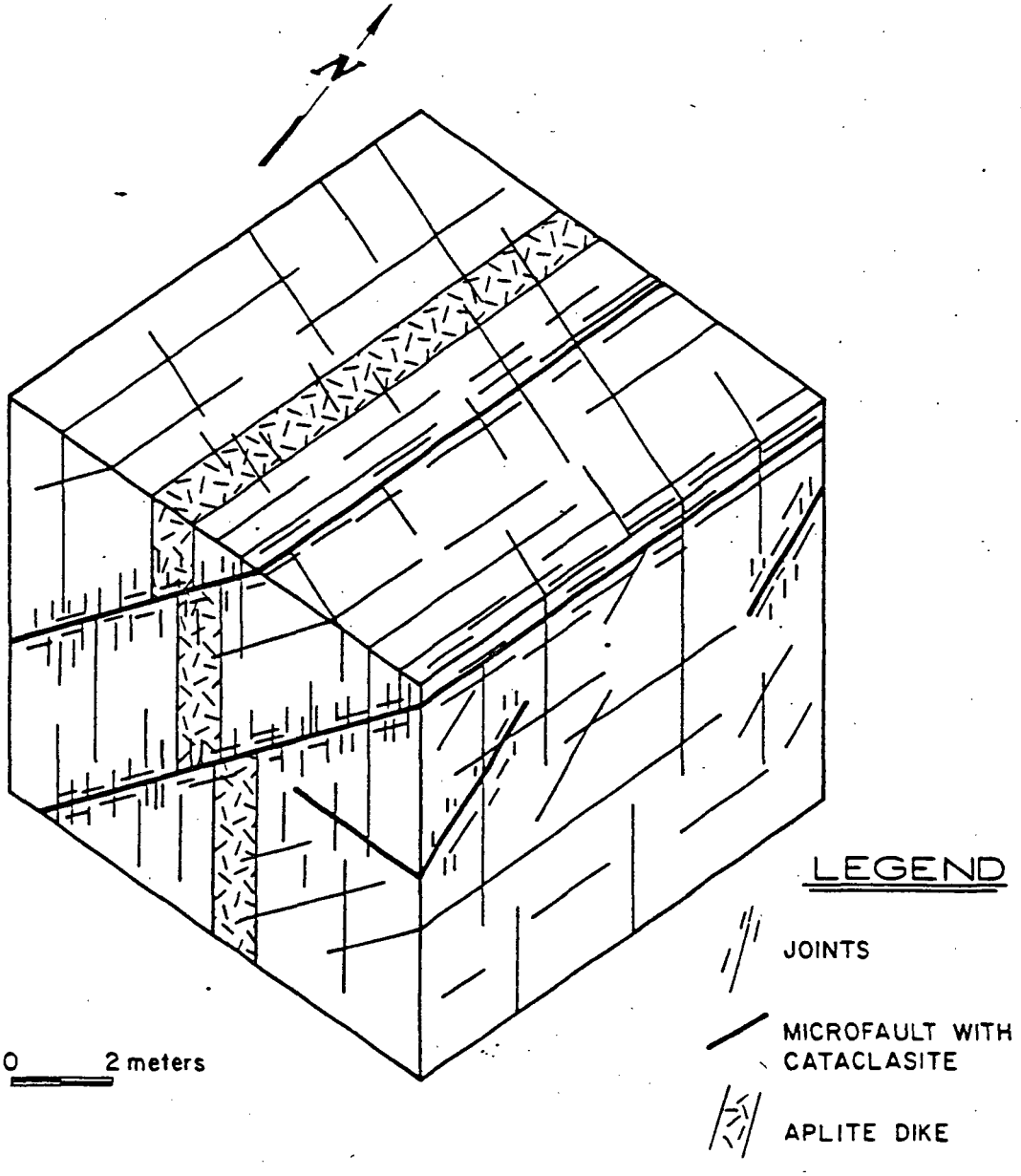

FIG. 5

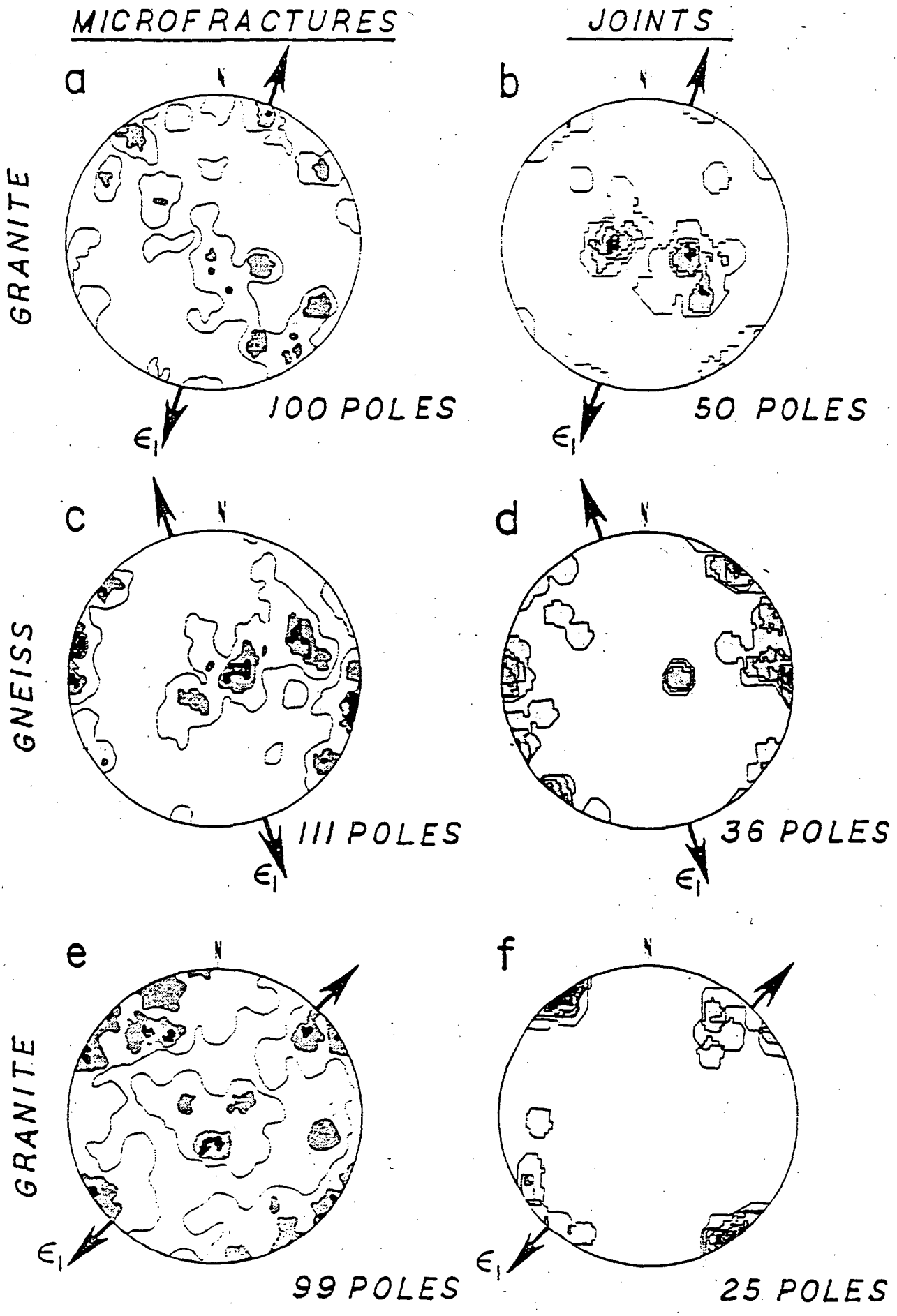
MICROFRACTURES
JOINTS
a
b
GRANITE
N
ϵ_1
100 POLES
50 POLES
c
d
GNEISS
111 POLES
36 POLES
e
f
GRANITE
99 POLES
25 POLES

MINERAL MOUNTAINS GRANITE
FAILURE ENVELOPE

TEST #	σ_3 (MPa)	σ_1 (MP
I	0	1.2
II	34	4.5
III	69	5.3

TENSILE STRENGTH
$T_0 = 5.0 \pm 2.4$ MPa

COHESIVE STRENG
$\tau_0 = 20$ MPa

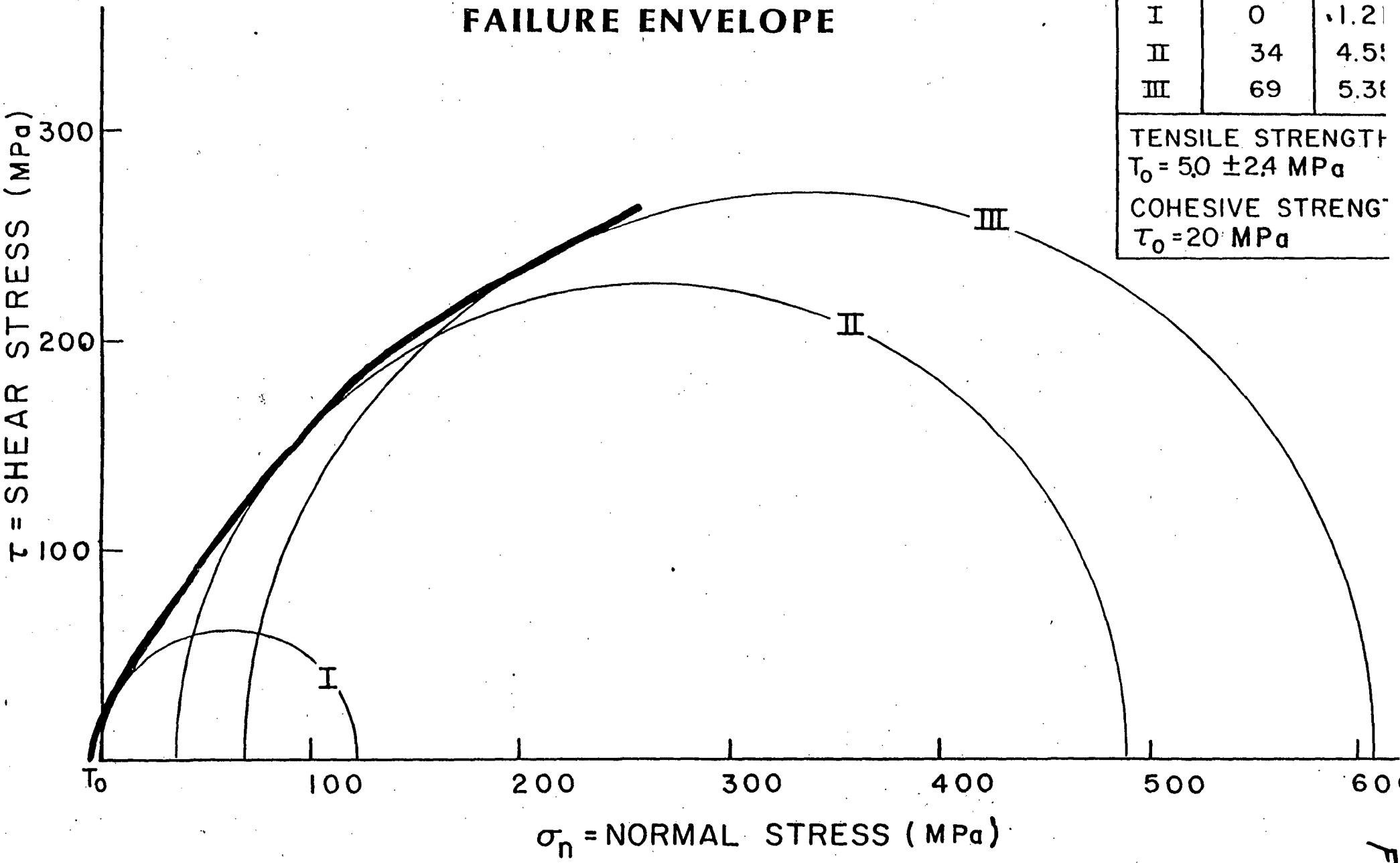

FIG. 6

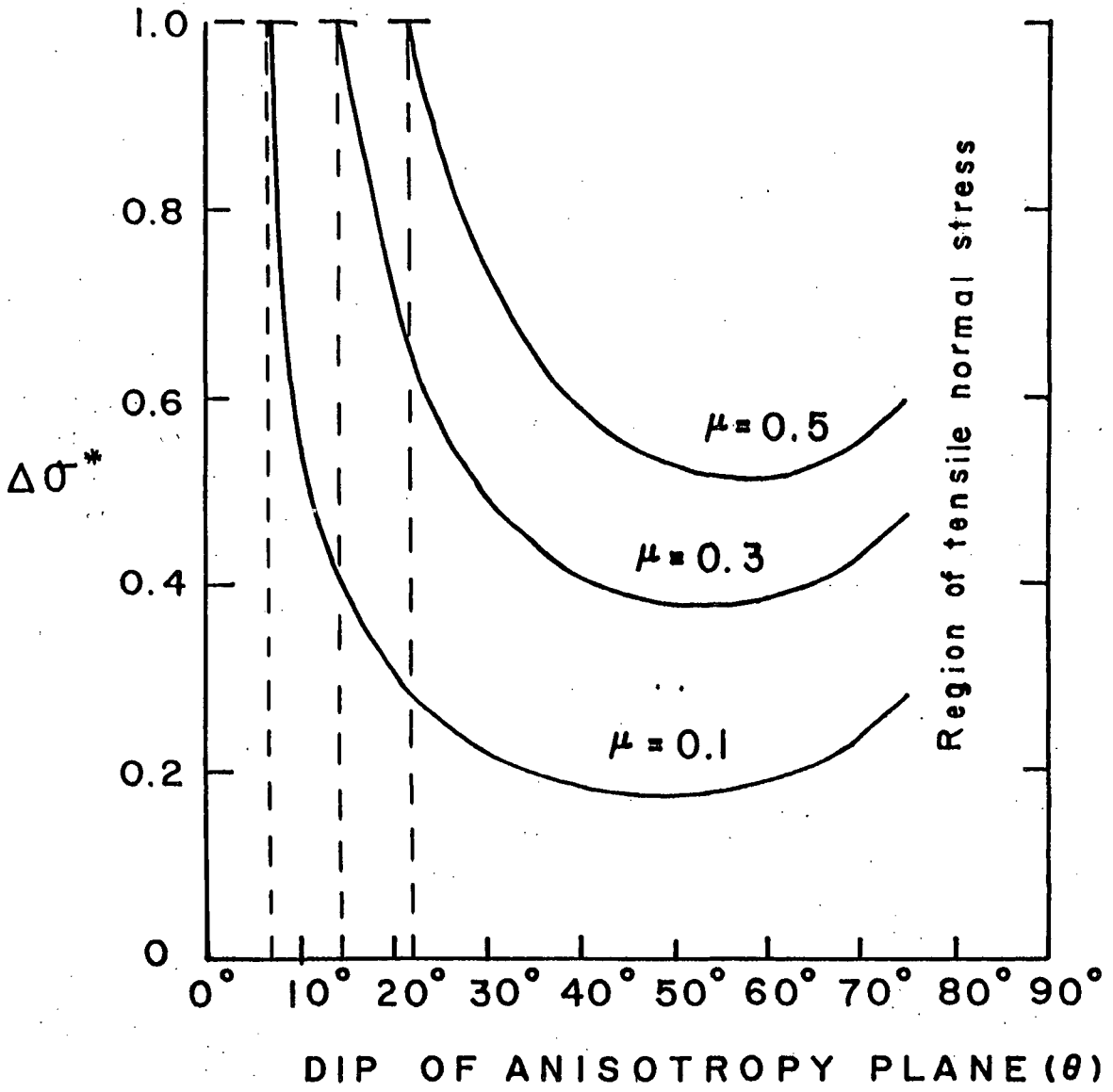

DEPTH = 2 Km.

FLUID PRESSURE = 125 % HYDROSTATIC

COHESION = 0

τmax = 1 MPa + 7 MPa/Km

$$\Delta\sigma^* = \frac{(\sigma_1 - \sigma_3)}{(\sigma_1 - \sigma_3)_c}$$

FIG. 7

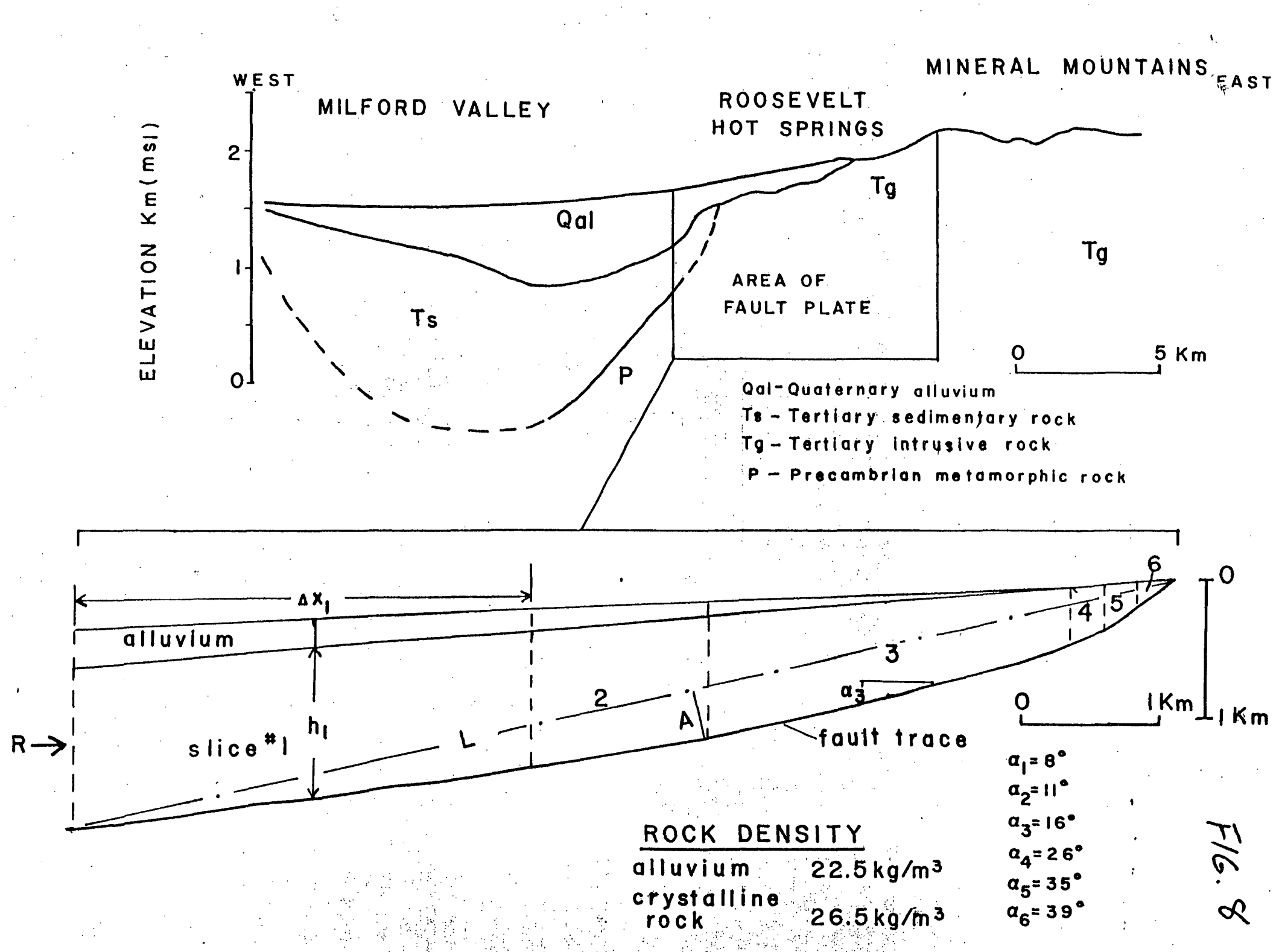
WEST
MILFORD VALLEY
ROOSEVELT HOT SPRINGS
MINERAL MOUNTAINS
EAST
ELEVATION Km(msl)
2
1
0
Qal
Ts
P
Tg
Tg
AREA OF FAULT PLATE
0
5 Km
Qal-Quaternary alluvium
Ts - Tertiary sedimentary rock
Tg - Tertiary intrusive rock
P - Precambrian metamorphic rock
ΔX1
alluvium
h1
slice #1
R
L
A
fault trace
1
2
3
4
5
6
α3
0
1Km
0
1Km
α1 = 8°
α2 = 11°
α3 = 16°
α4 = 26°
α5 = 35°
α6 = 39°
ROCK DENSITY
alluvium 22.5 kg/m3
crystalline rock 26.5 kg/m3

Fig. 8